Supplementary Information for

The innate immune protein human calprotectin induces iron starvation responses in *Pseudomonas aeruginosa*

Emily M. Zygiel[1], Cassandra E. Nelson[2], Luke K. Brewer[2], Amanda G. Oglesby-Sherrouse[2,3], Elizabeth M. Nolan[1,]

[1] Department of Chemistry, Massachusetts Institute of Technology, Cambridge, MA 02139, USA
[2] School of Pharmacy, Department of Pharmaceutical Sciences, University of Maryland, Baltimore, MD 21201, USA
[3] School of Medicine, Department of Microbiology and Immunology, University of Maryland, Baltimore, MD, 21021, USA

Running title: *Calprotectin induces iron starvation in* Pseudomonas aeruginosa

Corresponding author: Elizabeth Nolan (lnolan@mit.edu, 617-452-2495) and Amanda G. Oglesby-Sherrouse (aoglesby@rx.umaryland.edu, 410-706-8650)

This PDF file includes:

Table of contents
Tables S1-S8
Figures S1-S13
References for SI reference citations

TABLE OF CONTENTS

Supplementary tables

Supplementary figures

SUPPLEMENTAL TABLES

Table S1. Strains and plasmids used in this study

Name	Description	Reference
Strains		
Escherichia coli SM10 λ*pir*/P_{antR}-'*lacZ*$^{-SD}$	*E. coli* strain used for conjugation: pirR6K carrying P_{antR}-'*lacZ*$^{-SD}$	(1)
Escherichia coli SM10/pFLP	SM10 carrying the pFLP recombinase	(2)
Pseudomonas aeruginosa PAO1	*Pa* laboratory strain	(3)
Pseudomonas aeruginosa PAO1 Δ*pvdA*	Deletion of *pvdA* generated in PAO1	(4)
Pseudomonas aeruginosa PAO1 Δ*prrF*	Deletion of *prrF* generated in PAO1	(5)
Pseudomonas aeruginosa PA14	Clinical isolate UCBPP-PA14	(6), Courtesy of Dianne Newman
Pseudomonas aeruginosa PA14 Δ*phz*	Deletion of *phzA1-G1* and *phzA2-G2* from PA14	(7), Courtesy of Dianne Newman
Pseudomonas aeruginosa PAO1/P_{antR}-'*lacZ*$^{-SD}$	PAO1 with the P_{antR}-'*lacZ*$^{-SD}$ reporter fusion integrated at the chromosomal *att* site	(1)
Pseudomonas aeruginosa Δ***prrF***/ P_{antR}-'*lacZ*$^{-SD}$	PAO1 Δ*prrF* with the P_{antR}-'*lacZ*$^{-SD}$ reporter fusion integrated at the chromosomal *att* site	(1)
Pseudomonas aeruginosa PA14/ P_{antR}-'*lacZ*$^{-SD}$	PA14 with the P_{antR}-'*lacZ*$^{-SD}$ reporter fusion integrated at the chromosomal *att* site	This study
Pseudomonas aeruginosa Δ*phz*/ P_{antR}-'*lacZ*$^{-SD}$	PA14 Δ*phz* with the P_{antR}-'*lacZ*$^{-SD}$ reporter fusion integrated at the chromosomal *att* site	This study
Staphylococcus aureus USA300 JE2	MRSA strain USA300 cured of three plasmids, Tet^S, Ery^S	NTML, (8)
Escherichia coli UTI89	Uropathogenic *E. coli* isolated from a patient with an acute bladder infection	Courtesy of Dr. L. Cegelski, (9)
Salmonella enterica Typhimurium ATCC 14028™	Isolated from pools of heart and liver from 4-week old chickens, serotype I 4,5,12:i:1,2	(10)

Klebsiella pneumoniae ATCC 13883™	Type 3 antigenic	(11)
Acinetobacter baumannii ATCC 17978™	Isolated from a case of fatal meningitis of a 4-month old infant	(12)
Plasmids		
Mini-CTX1-P_{antR}-*lacZ*-SD	Integration-proficient plasmid Mini-CTX1-*lacZ* with the Shine-Dalgarno site deleted and the *antR* promoter cloned into the MCS	(1)

Table S2. Primers and probes used for RT-PCR

Oligonucleotide	Sequence 5'– 3'	Reference
Primers		
pvdS.for	CCT GGT CAA CTT CAT GAT CCG	(13)
pvdS.rev	AGA TGG GTG ACG TTG TCG	(13)
oprF.for	GCG TTC GCA ACA TGA AGA AC	(14)
oprF.rev	CTT CTT GTT GCC GGT TTC GTA	(14)
Probes		
pvdS	CCT GGT GCA CTG CCG CAA GGT	(13)
oprF	CGG TGA GTA CCA TGA CGT TCG TGG C	(14)

Table S3. Nomenclature of human calprotectin variants

Protein	S100A8 Mutation(s)	S100A9 Mutation(s)	Description
CP	N/A	N/A	Wild-type (WT)
CP-Ser	C42S	C3S	Cys → Ser variant
CP-Ser ΔHis$_3$Asp	C42S, H83A, H87A	C3S, H20A, D30A	Functional His_6 site
CP-Ser ΔHis_4	C42S, H17A, H27A	C3S, H91A, H95A	Functional His_3Asp site
CP-Ser ΔΔ	C42S, H17A, H27A, H83A, H87A	C3S, H20A, D30A, H91A, H95A	No functional transition-metal-binding sites

Table S4. Representative metal analysis of Tris:TSB medium

Element	ppb	µM
Mg	2246	184.8
Ca*	57720	2880
Mn	5.349	0.1947
Fe	106.2	3.805
Co	1.522	0.05165
Ni	8.092	0.2757
Cu	3.694	0.1162
Zn	172.8	5.286

*Contains a 2 mM Ca(II) supplement

Table S5. Representative metal analysis of metal-depleted Tris:TSB

Element	ppb	µM
Mg	2970	122.2
Ca*	88820	2216
Mn	3.585	0.06526
Fe	39.69	0.7106
Co	1.660	0.02818
Ni	46.56	0.7933
Cu	3.080	0.04847
Zn	42.89	0.6559

*Contains a 2 mM Ca(II) supplement

Table S6. Average OD_{600} values for biological replicates from Figure 2

Culture treatment	OD_{600} ± SDM*
Replete (A)	2.4 ± 0.3
Depleted (A)	1.6 ± 0.1
Mn-depleted (A)	2.5 ± 0.1
Fe-depleted (A)	1.8 ± 0.1
Zn-depleted (A)	2.4 ± 0.3
Replete + CP-Ser (A)	2.1 ± 0.3
Untreated (B)	2.3 ± 0.2
CP-Ser (B)	1.9 ± 0.1
ΔHis_3Asp (B)	2.0 ± 0.2
ΔHis_4 (B)	2.6 ± 0.4
ΔΔ (B)	2.5 ± 0.4

* N = 3 (A), N = 4 (B), SDM

Table S7. Representative metal analysis of LB medium

Element	ppb	µM
Mg	945.1	77.75
Ca	2983	148.9
Mn	7.546	0.2747
Fe	220.3	7.888
Co	4.836	0.1641
Ni	0.000	0.000
Cu	6.812	0.2144
Zn	509.0	15.57

Table S8. Metal analysis of purified pyoverdine (10 µM sample)

Element	ppb	µM
Mg	12.439	0.512
Ca	93.693	2.338
Mn	0.577	0.011
Fe	1.715	0.031
Co	0.361	0.006
Ni	0.000	0.000
Cu	0.134	0.002
Zn	2.296	0.035

SUPPLEMENTAL FIGURES

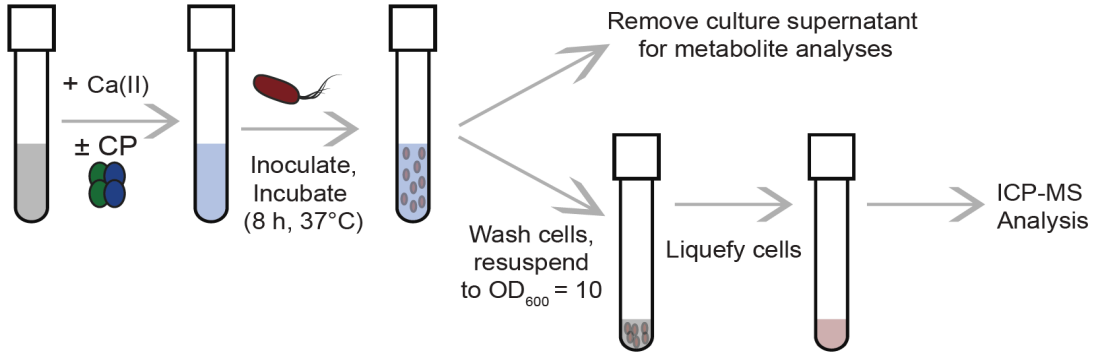

Figure S1. Experimental setup for metal inventory and metabolite analyses. Medium containing 2 mM Ca(II) was supplemented with or without CP. The medium was inoculated with an overnight culture of bacteria (1:100 dilution) and grown for 8 hours at 37°C. After centrifugation, the supernatant was isolated for metabolite analyses, and the cells were washed and re-suspended to an OD_{600} = 10. This bacterial suspension was liquefied and its metal content was analyzed by ICP-MS.

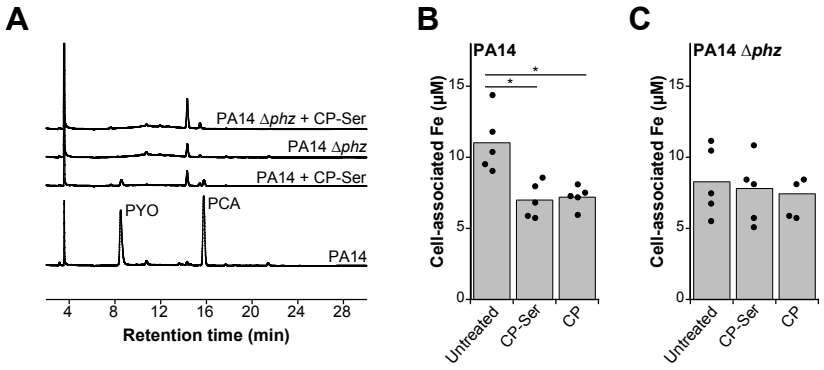

Figure S2. Effect of CP on iron uptake by *P. aeruginosa* PA14 and Δ*phz*. (A) HPLC chromatograms (365 nm absorption) for culture supernatants of PA14 and PA14 Δ*phz*. PYO and PCA are labeled in the PA14 supernatant. (B and C) Cell-associated iron of (B) PA14 and (C) Δ*phz*. Cultures were grown in Tris:TSB in the absence or presence of CP-Ser or wild-type CP (10 μM) at 37°C for 8 h. Cell-associated metal levels correspond to the concentration of metal in a liquefied suspension of cells at an OD_{600} of 10. Untreated and CP-Ser data are re-produced for comparison (N = 4 for Δ*phz* treated with CP, N = 5 for all other conditions, $*P < 0.05$).

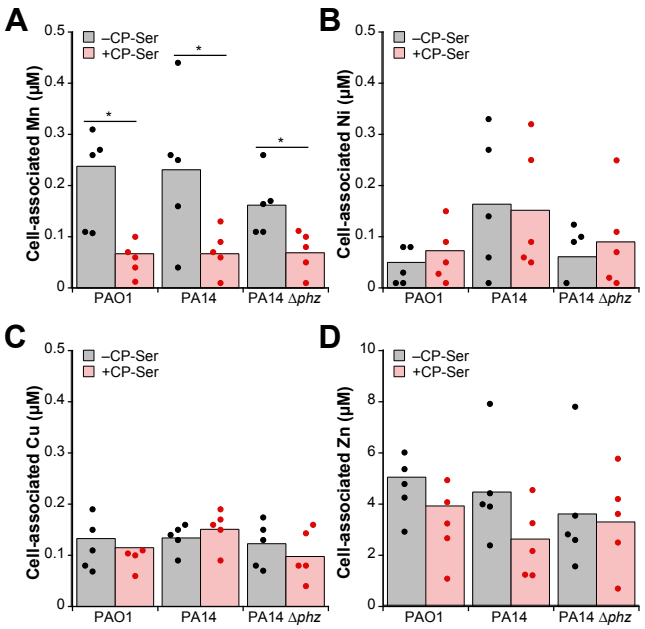

Figure S3. CP inhibits manganese, but not nickel, copper, or zinc, uptake by *P. aeruginosa.* PA01, PA14, and PA14 Δ*phz* were grown in Tris:TSB the absence or presence of CP-Ser (10 μM) at 37°C for 8 h. Cell-associated metal levels correspond to the concentration of metal in a liquefied suspension of cells at an OD_{600} of 10 (N = 5, **P* < 0.05).

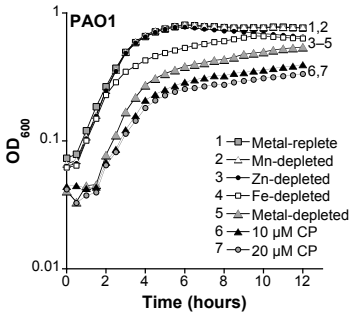

Figure S4. CP and iron-depletion are growth inhibitory to *P. aeruginosa* PAO1. PAO1 was grown in metal-depleted Tris:TSB in the absence or presence of CP-Ser (10 or 20 μM) at 37°C for 12 h (N = 3, error bars are SE).

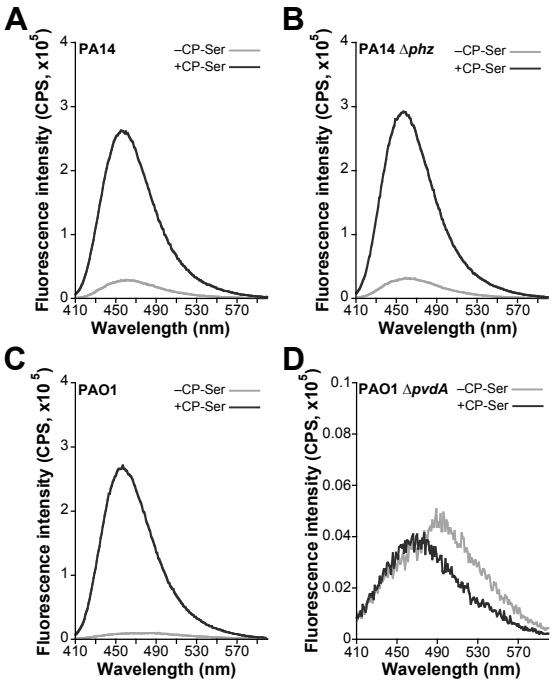

Figure S5. Effect of CP on pyoverdine fluorescence. *P. aeruginosa* PAO1, PAO1 Δ*pvdA*, PA14, and PA14 Δ*phz* were grown in the absence or presence of CP-Ser (10 μM) at 37°C for 8 h. Supernatant was diluted 1:10 into 50 mM Tris pH 8.0 before measuring fluorescence (λ_{ex} = 400 nm). Three biological replicates were performed and representative emission spectra are shown.

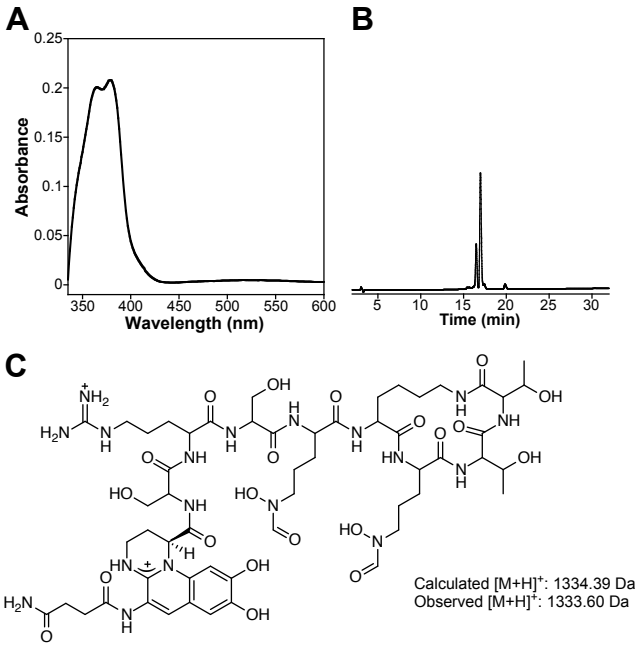

Figure S6. Purified pyoverdine from *P. aeruginosa* PAO1. (A) Optical absorption spectrum of purified pyoverdine (~15 μM) in 50 mM acetate pH 5.0. The observed spectrum corresponds to apo pyoverdine at pH 5.0 as previously reported.(15) (B) HPLC chromatogram (220 nm) of purified pyoverdine. The major peak is pyoverdine, which is in 56% purity. (C) Mass spectrometry of purified pyoverdine afforded an observed $[M+H]^+$ of 1333.60 Da, which is in agreement with the calculated $[M+H]^+$ of 1334.39 Da for pyoverdine PVD1 modified with a succinamide group.(16)

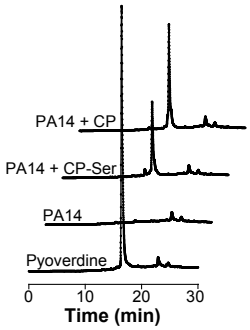

Figure S7. Effect of CP-Ser and wild-type CP on pyoverdine production. HPLC fluorescence detection (λ_{ex} = 398 nm and λ_{em} = 455 nm) for *P. aeruginosa* PA14 cultures grown in the absence or presence of CP-Ser or CP (10 µM) at 37°C for 8 h. The pyoverdine standard was run at a concentration of 50 µM. Three biological replicates were performed and representative results are shown. Average OD_{600} values (mean ± SDM, N = 3) for cultures were 2.3 ± 0.2 (PA14), 2.0 ± 0.1 (PA14 + CP-Ser) and 1.9 ± 0.1 (PA14 + CP).

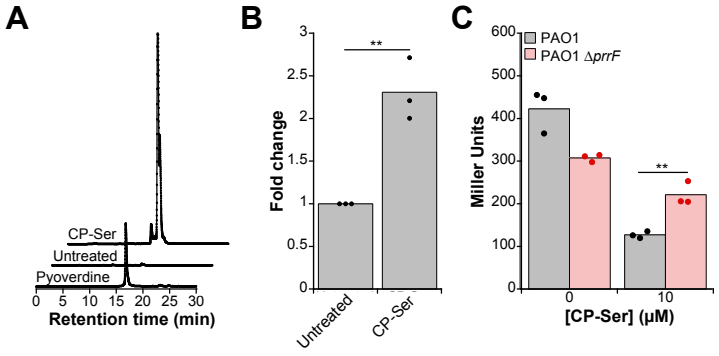

Figure S8. CP promotes pyoverdine production and *pvdS* transcription, and inhibits *antR* translation in CDM. All cultures were grown in CDM at 37°C for 16 h. (A) HPLC fluorescence detection (λ_{ex} = 398 nm and λ_{em} = 455 nm) for pyoverdine in *P. aeruginosa* PAO1 cultures grown in CDM in the absence or presence of CP-Ser (10 µM). Three biological replicates were performed and representative results are shown. Average OD_{600} values (mean ± SDM, N = 3) for cultures were 8.2 ± 0.5 (PAO1) and 6.2 ± 0.7 (PAO1 + CP-Ser). (B) RT-PCR analysis of *pvdS* mRNA levels in PAO1 grown in the absence or presence of CP-Ser (10 µM). mRNA levels were normalized to *oprf* and the fold change relative to the untreated condition is presented (N = 3, $^{**}P < 0.01$). (C) *antR* translation in PAO1/P_{antR}-'*lacZ*$^{-SD}$ and Δ*prrF*/P_{antR}-'*lacZ*$^{-SD}$ after growth in the absence or presence of CP-Ser (10 µM). β-Galactosidase activity was assayed in cell suspensions (N = 3, $^{**}P < 0.01$).

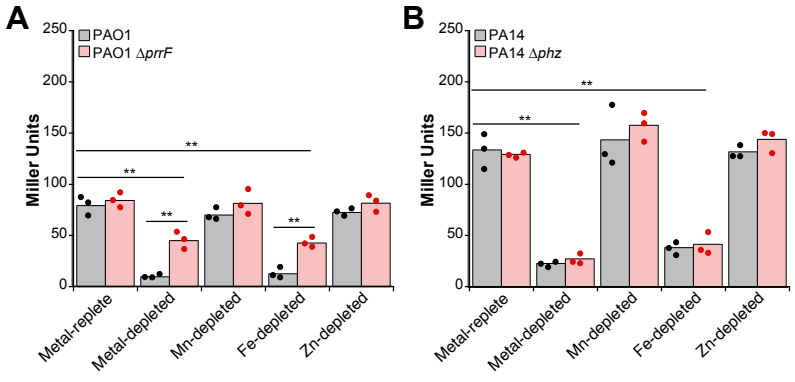

Figure S9. Iron depletion inhibits *antR* translation. *P. aeruginosa* (A) PAO1/P_{antR}-'*lacZ*^{SD} and Δ*prrF*/P_{antR}-'*lacZ*^{SD} and (B) PA14/P_{antR}-'*lacZ*^{SD} and PA14 Δ*phz*/P_{antR}-'*lacZ*^{SD} were grown in metal-depleted Tris:TSB in the absence or presence of 10 μM CP-Ser at 37°C for 8 h. β-Galactosidase activity was assayed in cell suspensions (N = 3, $^{**}P < 0.01$).

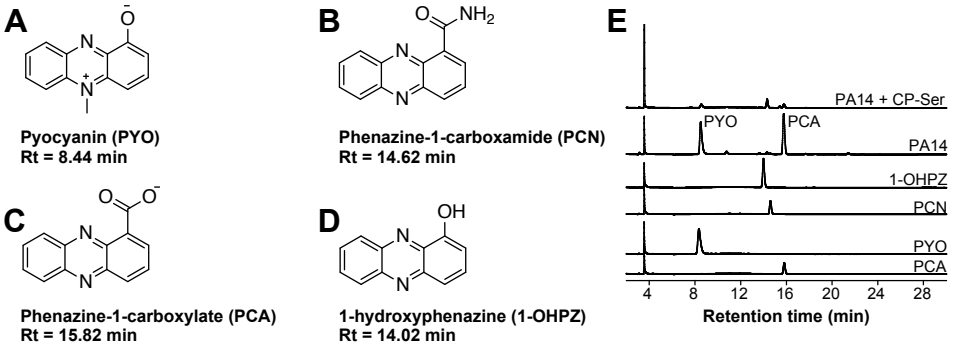

Figure S10. Structures and retention times (Rt) of phenazines. Structure of PYO (A), phenazine-1-carboxamide (PCN, B), PCA (C), and 1-hydroxyphenazine (1-OHPZ, D). (E) Chromatograms (365 nm) of phenazine standards and phenazines detected in supernatants from *P. aeruginosa* PA14 cultures grown in Tris:TSB in the absence or presence of CP-Ser (10 μM) at 37°C for 8 h. Standards were run at 50 μM (PYO and 1-OHPZ) or 10 μM (PCA and PCN).

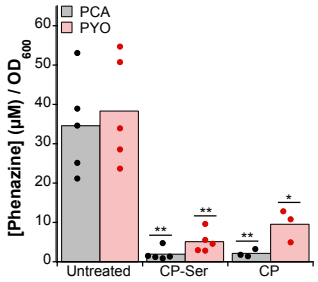

Figure S11. CP-Ser and wild-type CP inhibit phenazine production. Average PCA and PYO concentration in supernatants from *P. aeruginosa* PA14 cultures grown in Tris:TSB the absence or presence of 10 μM CP-Ser or CP at 37°C for 8 h. Phenazine concentrations were determined using a standard curve and have been normalized to the OD_{600} of their respective cultures. Culture OD_{600} ranged from 1.7–2.5 (N = 5 for Untreated and CP-Ser, N = 3 for CP,*$P < 0.05$, **$P < 0.01$ for comparison to the untreated condition).

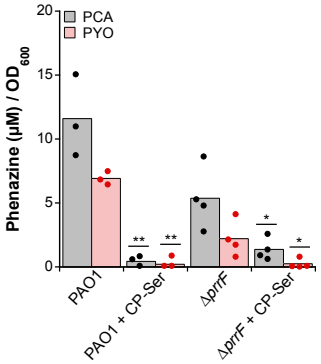

Figure S12. PrrF sRNAs are not required for inhibition of phenazine production by CP. Average PCA and PYO concentration in supernatants from *P. aeruginosa* PAO1 and PAO1 Δ*prrF* cultures grown in Tris:TSB the absence or presence of 10 μM CP-Ser at 37°C for 8 h. Phenazine concentrations were determined using a standard curve and have been normalized to the OD_{600} of their respective cultures. Culture OD_{600} ranged from 2.6–3.0 in untreated cultures and 1.5–2.0 in cultures treated with CP-Ser (N = 3 for PAO1, N = 4 for PAO1 Δ*prrF*, * $P < 0.05$, **$P < 0.01$ for comparison to respective untreated cultures).

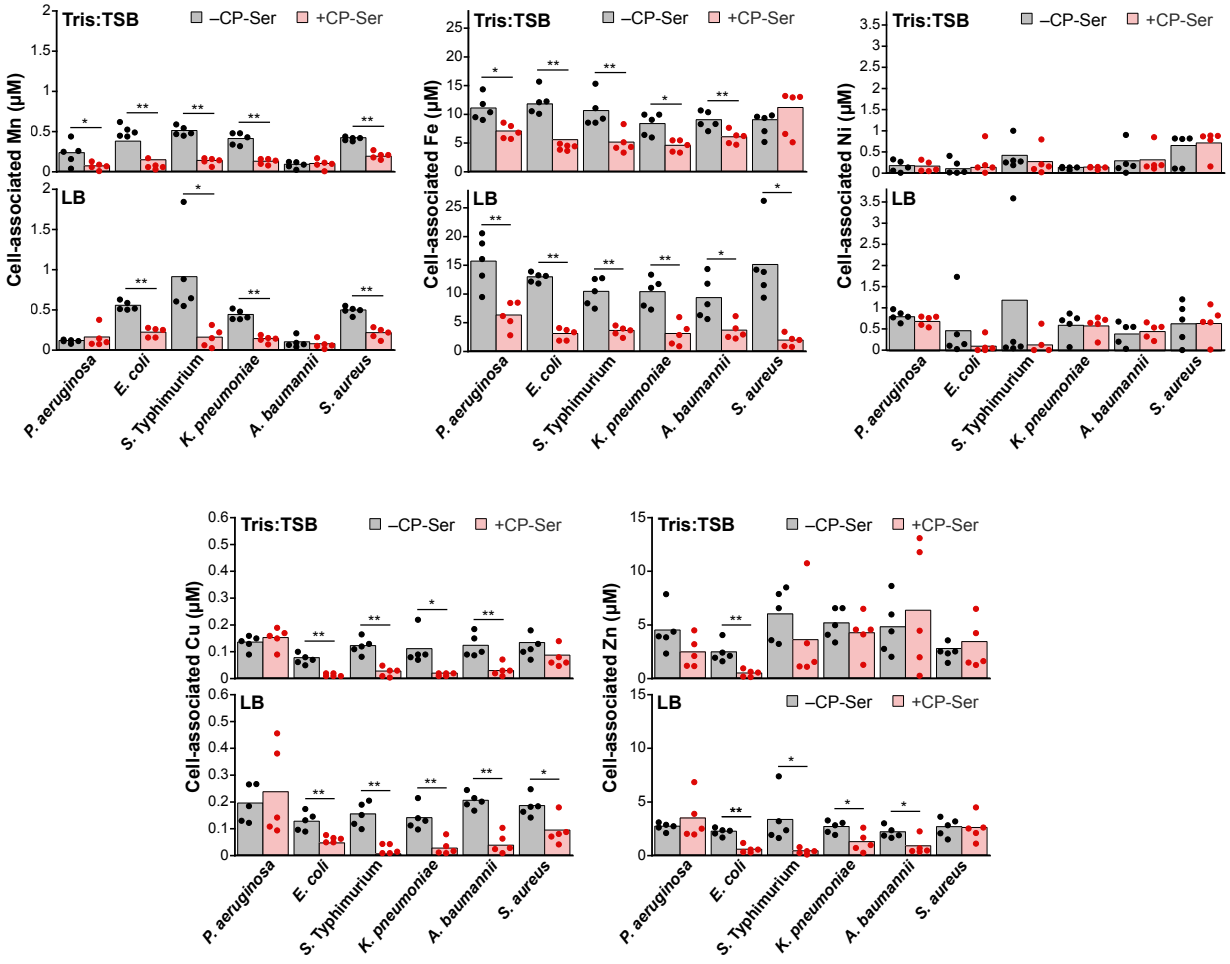

Figure S13. CP inhibits manganese, iron, nickel, copper, and zinc uptake by bacterial pathogens. *P. aeruginosa* PA14, *Staphylococcus aureus* USA300 JE2, *Escherichia coli* UTI89, *Salmonella enterica* Typhimurium ATCC 14028, *Klebsiella pneumoniae* ATCC 13883, and *Acinetobacter baumannii* ATCC 17978 were grown in LB or Tris:TSB in the absence or presence of 10 μM CP-Ser (for cultures in Tris:TSB) or 20 μM CP-Ser (for cultures in LB) at 37°C for 8 h. Cell-associated iron corresponds to the concentration of Fe in an OD_{600} = 10.0 cell suspension (N = 5, *$P < 0.05$; **$P < 0.01$). The cell-associated iron data (panel B) from Figure 7 of the main text are included for comparison.

SUPPORTING REFERENCES

1. Djapgne, L., Panja, S., Brewer, L. K., Gans, J. H., Kane, M. A., Woodsen, S. A., and Oglesby-Sherrouse, A. G. (2018) The *Pseudomonas aeruginosa* PrrF1 and PrrF2 small regulatory RNAs promote 2-alkyl-4-quinolone production through redundant regulation of the *antR* mRNA. *J. Bacteriol.* **200**, 00704-17
2. Hoang, T. T., Karkhoff-Schweizer, R. R., Kutchma, A. J., and Schweizer, H. P. (1998) A broad-host-range Flp-FRT recombination system for site-specific excision of chromosomally-located DNA sequences: application for isolation of unmarked *Pseudomonas aeruginosa* mutants. *Gene* **212**, 77-86
3. Holloway, B. W. (1955) Genetic recombination in *Pseudomonas aeruginosa. J. Gen. Microbiol.* **13**, 572-581
4. Ochsner, U. A., Vasil, A. I., and Vasil, M. L. (1995) Role of the ferric uptake regulator of *Pseudomonas aeruginosa* in the regulation of siderophores and exotoxin A expression: purification and activity on iron-regulated promoters. *J. Bacteriol.* **177**, 7194-7201
5. Wilderman, P. J., Sowa, N. A., FitzGerald, D. J., Fitzgerald, P. C., Gottesman, S., Ochsner, U. A., and Vasil, M. L. (2004) Identification of tandem duplicate regulatory small RNAs in *Pseudomonas aeruginosa* involved in iron homeostasis. *Proc. Nat. Acad. Sci. U.S.A.* **101**, 9792-9797
6. Rahme, L. G., Stevens, E. J., Wolfort, S. F., Shao, J., Tompkins, R. G., and Ausubel, F. M. (1995) Common virulence factors for bacterial pathogenicity in plants and animals. *Science* **268**, 1899-1902
7. Dietrich, L. E., Price-Whelan, A., Petersen, A., Whiteley, M., and Newman, D. K. (2006) The phenazine pyocyanin is a terminal signalling factor in the quorum sensing network of *Pseudomonas aeruginosa*. *Mol. Microbiol.* **61**, 1308-1321
8. Fey, P. D., Endres, J. L., Yajjala, V. K., Widhelm, T. J., Boissy, R. J., Bose, J. L., and Bayles, K. W. (2013) A genetic resource for rapid and comprehensive phenoype screening of nonessential *Staphylococcus aureus* genes. *MBio* **4**, e00537-12
9. Chen, S. L., Hung, C. S., Xu, J., Reigstad, C. S., Magrini, V., Sabo, A., Blasiar, D., Bieri, T., Meyer, R. R., Ozersky, P., Armstrong, J. R., Fulton, R. S., Latreille, J. P., Spieth, J., Hooton, T. M., Mardis, E. R., Hultgren, S. J., and Gordon, J. I. (2006) Identification of genes subject to positive selection in uropathogenic strains of *Escherichia coli*: a comparative genomics approach. *Proc. Nat. Acad. Sci. U.S.A.* **103**, 5977-5982
10. Fields, P. I., Swanson, R. V., Haidaris, C. G., and Heffron, F. (1986) Mutants of *Salmonella typhimurimum* that cannot survive within the macrophage are avirulent. *Proc. Nat. Acad. Sci. U.S.A.* **83**, 5189-5193
11. Cowan, S. T., Steel, K. J., Shaw, C., and Duguid, J. P. (1960) A classification of the *Klebsiella* group. *J. Gen. Microbiol.* **23**, 601-612
12. Baumann, P., Doudoroff, M., and Stanier, R. Y. (1968) A study of the *Moraxella* group. II. Oxidative-negative species (genus *Acinetobacter*). *J. Bacteriol.* **95**, 1520-1541
13. Nguyen, A. T., O'Neill, M. J., Watts, A. M., Robson, C. L., Lamont, I. L., Wilks, A., and Oglesby-Sherrouse, A. G. (2014) Adaptation of iron homeostasis pathways by a *Pseudomonas aeruginosa* pyoverdine mutant in the cystic fibrosis lung. *J. Bacteriol.* **196**, 2265-2276
14. Reinhart, A. A., Nguyen, A. T., Brewer, L. K., Bevere, J., Jones, J. W., Kane, M. A., Damron, F. H., Barbier, M., and Oglesby-Sherrouse, A. G. (2017) The *Pseudomonas aeruginosa* PrrF small RNAs regulate iron homeostasis during acute murine lung infection. *Infect. Immun.* **85**, e00764-16
15. Xiao, R., and Kisaalita, W. S. (1995) Purification of pyoverdines of *Pseudomonas fluorescens* 2-79 by copper-chelate chromatography. *Appl. Environ. Microbiol.* **61**, 3769-3774
16. Briskot, G., Taraz, K., and Budzikiewicz, H. (1986) Pyoverdin-type siderophores from *Pseudomonas aeruginosa*. *Z. Naturforsch C.* **41**, 497-506